

# BIFACIAL pSPEER SOLAR CELLS FOR SHINGLE MODULES

P. Baliozian, T. Fellmeth, N. Wöhrle, E. Lohmüller, R. Preu  
Fraunhofer Institute for Solar Energy Systems ISE, Heidenhofstr. 2, 79110 Freiburg, Germany  
Phone: +49 761 - 4588 5383; e-mail: puzant.baliozian@ise.fraunhofer.de

**ABSTRACT:** Shingling bifacial solar cells leads to higher output power densities  $p_{\text{out}}$  of silicon-based photovoltaic modules. This paper provides a short update on the current developments at Fraunhofer ISE in Czochralski-grown silicon bifacial “p-type shingled passivated edge, emitter, and rear (pSPEER)” solar cells. In the batch presented in this work, conventionally separated pSPEER cells are fabricated. Illuminated current-voltage measurements of the most efficient pSPEER cell results in a designated front side energy conversion efficiency of  $\eta_f = 21.4\%$  for an irradiance  $G_f = 1000 \text{ W/m}^2$ . The pSPEER cells show similar front side efficiencies independent of the pre-separation position within the 6-inch host wafer. Considering an additional rear side irradiance of  $G_r = 100 \text{ W/m}^2$ , the most efficient pSPEER cell attains a total designated output power density  $p_{\text{out}} = 22.8 \text{ mW/cm}^2$ .

**Keywords:** bifacial, p-type silicon, PERC, pSPEER, shingle solar cells

## 1 INTRODUCTION

Although the idea of shingling solar cells exists since the 1950s [1], it was only used for niche applications [2]. The aim towards achieving high output power density  $p_{\text{out}}$  modules has revived the concept of shingling, clearly seen in the increase in the number of recent publications [3], patents [4], and commercially available monofacial modules [5] based on shingling interconnection. In the case of shingling (overlapping) interconnection of solar cells, the rear side busbar of a cell overlaps the front busbar of the neighboring cell. Consequently, the active area within the module increases by omitting the spacing between the cells as well as eliminating the shadowing losses from the busbars covered by the neighboring cell’s active area. Additionally, shingling interconnection decreases resistive losses on module level decreasing cell-to-module losses.

An additional gain in  $p_{\text{out}}$  can be attained by using bifacial solar cells that make use of the albedo light from the surroundings. Moreover, the p-type silicon passivated emitter and rear cell (PERC) [6] concept is of high interest for the industry, which is clearly shown by the recent and expected increase in market share [7]. Thus, joining the concepts of shingling, bifaciality and the state-of-the-art PERC technology provides industry relevant solutions for modules with high  $p_{\text{out}}$ .

This paper aims to portray recent developments in the bifacial “p-type shingled passivated edge, emitter, and rear (pSPEER)” solar cells that have been first introduced in Ref. [8]. The current fabrication process at Fraunhofer ISE and characterization results of pSPEER cells are discussed.

## 2 pSPEER SOLAR CELL FABRICATION AND CHARACTERIZATION

### 2.1 Fabrication Process

Currently, pSPEER solar cells are fabricated by using industrial 6-inch Czochralski-grown silicon (Cz-Si) precursors with rear and front side passivation layers that undergo the backend processes; see Fig. 1. In this work the 6-inch p-type Cz-Si precursors used feature a phosphorous oxychloride diffused n-type emitter. The rear and front sides are passivated by a industrial typical stack of aluminum oxide and silicon nitride. In a previously performed batch, similar precursors’ mean

thickness  $t$  is measured to be  $t = 155 \mu\text{m}$  and the base resistivity  $\rho_B$  is measured to be ranging between  $0.3 - 0.9 \Omega\text{cm}$ . The mean measured implied open-circuit voltage is  $iV_{\text{OC}} = 702 \text{ mV}$ . For the formation of the local contact openings (LCO), an infrared laser process is used to locally ablate the rear side passivation layer. The rear and front side metallization layouts are printed by using commercial metal pastes in an industrial-type screen printing line. Initially, the rear side silver busbars are printed, followed by the rear side aluminum finger grid covering the LCO. Subsequently, the front side silver finger grid is printed and then contact fired in an industrial fast firing process at set peak temperatures around  $840 \text{ }^\circ\text{C}$ . After firing, the rear side silver busbar features a mean measured width  $w \approx 492 \mu\text{m}$ . The mean rear side aluminum finger width is measured to be  $w \approx 221 \mu\text{m}$ , with a finger mid-to-mid pitch  $f_p = 1.3 \text{ mm}$ . The mean front side silver busbar is  $w \approx 800 \mu\text{m}$  wide, while the measured mean finger width is  $w \approx 37 \mu\text{m}$  having the pitch  $f_p = 1.3 \text{ mm}$  (details concerning the pSPEER metallization layouts can be found in Ref. [10].) Conventional laser scribing and manual cleaving is used to obtain 6 pSPEER cells from each host wafer. During this separation process approximately  $1/3^{\text{rd}}$  of the host wafer’s thickness is scribed using a pulsed laser and the rest is manually cleaved. The pSPEER cell has the perimeter dimensions:  $22 \text{ mm} \times 148 \text{ mm}$ ; see Fig. 2. These dimensions have been chosen to be compatible on the different industrially available wafer formats. In an industrial production of these cells, a format which utilizes the host wafer more efficiently would be used.

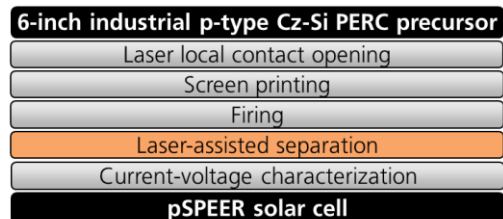


**Figure 1:** pSPEER solar cells backend fabrication processes starting from industrial 6-inch p-type Cz-Si PERC precursors (figure adapted from Ref. [9]).

## 2.2 Current-voltage measurement

The increased interest in cells ready for shingling interconnection also raises the questions of suitable current-voltage (*IV*) characterization for such shingle cells. Since the busbars of shingle cells are meant to be covered due to the overlap of the shingling interconnection, a designated area measurement (i.e. excluding busbar area) is also of interest. A total area measurement can be done and subsequently converted to a designated area. A calculation step by using the linear equation (1), converts total area short-circuit current  $I_{SC,tot}$ , into designated area short-circuit current density  $j_{SC,des}$  by only subtracting the busbar area  $A_{BB}$  from the total area  $A_{tot}$  of the pSPEER solar cell.

$$j_{SC,des} = \frac{I_{SC,tot}}{A_{tot} - A_{BB}} \quad (1)$$

The measured total area *IV* parameters of shingle pSPEER cells can be converted into designated area *IV* parameters without inducing errors larger than usual measurement deviations in *IV* testing. An elaboration on the difference between a total area and a designated area measurement of pSPEER cells will be given in Ref. [11].

For the *IV* measurements of pSPEER cells shown in this work, an industrial cell tester is used. The pSPEER cells are measured at standard test conditions subsequently from either side with an irradiance of  $G_f = 1000 \text{ W/m}^2$  placed on a conductive copper chuck. The full area measurement is done by fully contacting the rear side by means of a conductive copper chuck. The front side is contacted by an *IV* pin array. The set-up is calibrated using pSPEER cells measured at Fraunhofer ISE CalLab PV Cells on a black non-reflective background. At an irradiance  $G_f = 1000 \text{ W/m}^2$ , the output power density  $p_{out}$  in “mW/cm<sup>2</sup>” and the energy conversion efficiency  $\eta$  in “%” have identical numerical values (for an explanation see Ref. [12]).

## 3 RESULTS AND DISCUSSION

The peak designated area front side efficiency  $\eta_f = 21.4\%$  is attained having an open-circuit voltage  $V_{OC} = 666 \text{ mV}$ , short-circuit current density  $j_{SC,des} = 40.2 \text{ mA/cm}^2$ , and fill factor  $FF = 79.8\%$ ; see Table I. A front side pseudo-fill factor  $pFF = 82.3\%$  is measured.  $j_{SC,des}$  is calculated by using equation (1) where the total short-circuit current density  $j_{SC,tot}$  is taken from the *IV* measurement results. The average total area of a pSPEER cell is measured to be  $A_{tot} = 3263 \text{ mm}^2$ . The same pSPEER cell’s rear side measurement shows a designated area rear side efficiency of  $\eta_r = 13.7\%$ . The rear side short-circuit current density is  $j_{SC,des} = 26.2 \text{ mA/cm}^2$ ,  $V_{OC} = 654 \text{ mV}$ , and  $FF = 79.7\%$ . Finally, the bifaciality factor  $\beta = \eta_r/\eta_f$  is calculated out of the respective designated efficiencies to be  $\beta = 0.64$ . Figure 3 shows the *IV* data measurement results of 54 measured pSPEER cells.

Considering an additional rear side illumination with an irradiance  $G_r = 100 \text{ W/m}^2$ , the pSPEER cell with the highest  $p_{out}$  attains a designated total output power density  $p_{out} = 22.8 \text{ mW/cm}^2$ .

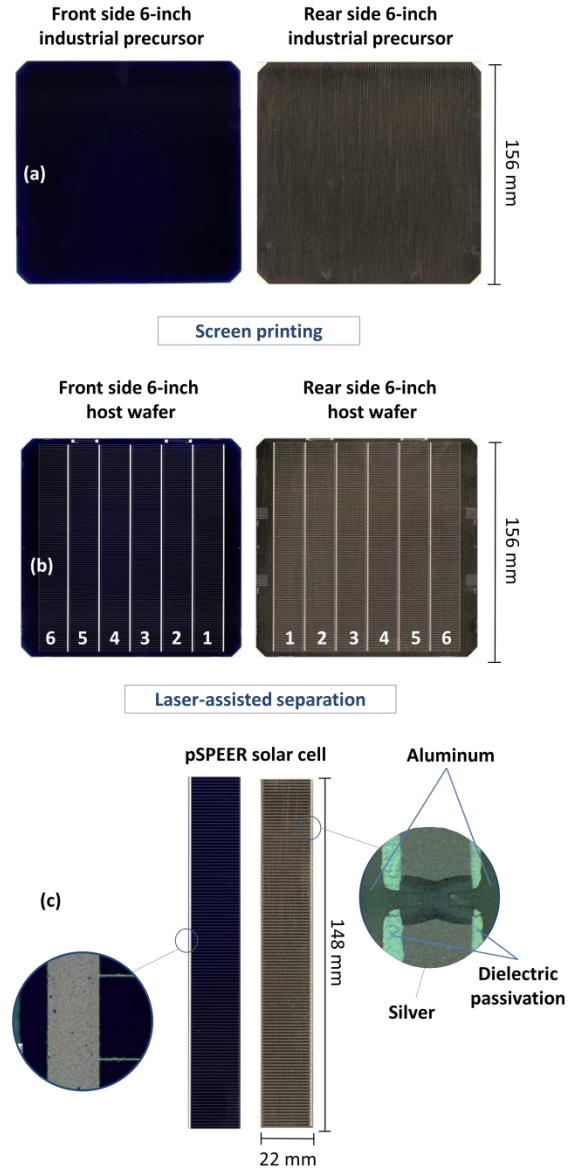


**Figure 2:** Images of the front and rear sides of (a) 6-inch industrial precursor (the rear side has a yellowish color since the precursor is optimized for monofacial use), (b) metallized host wafer after screen printing and (c) pSPEER solar cells of size 22 mm x 148 mm after separation.

**Table I:** *IV* data for the pSPEER solar cell with the highest output power density.

Meas. side	$\eta$ (%)	$V_{OC}$ (mV)	$j_{SC,des}$ (mA/cm <sup>2</sup> )	$FF$ (%)	$\beta$ (1)
Front	21.4	666	40.2	79.8	0.64
Rear	13.7	654	26.2	79.7	

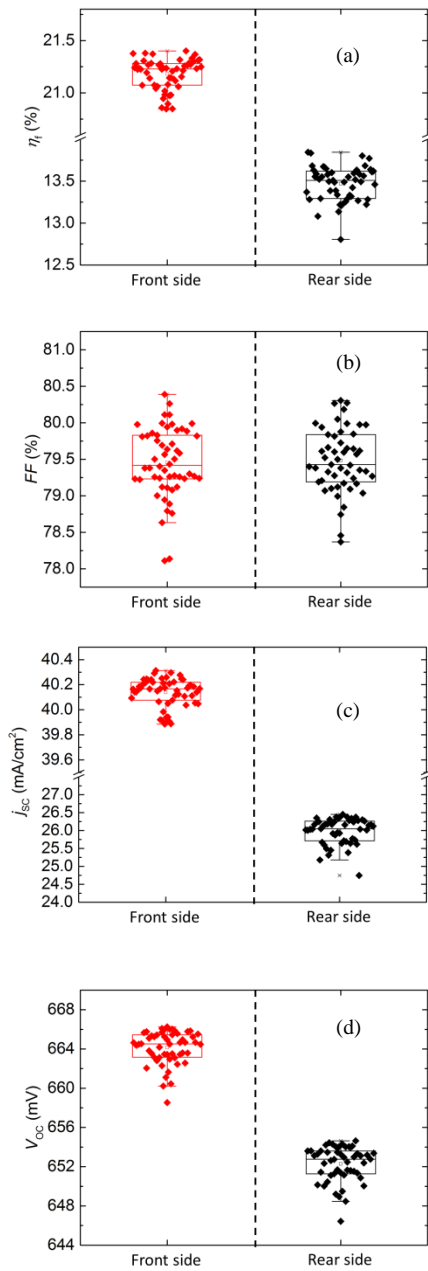


**Figure 3:** Front side and rear side *IV* measurement data of 54 pSPEER solar cells showing: (a) designated front side efficiency  $\eta_f$ , (b) fill factor  $FF$  (c) designated short-circuit current density  $j_{SC,des}$ , and (d) open-circuit voltage  $V_{OC}$ .

The dependency of  $\eta_f$  on their position pre-separated pSPEER cell within the host wafer is investigated. The designated front side efficiency  $\eta_f$  shows no significant difference in the range of results dependent on the position; see Fig. 4.

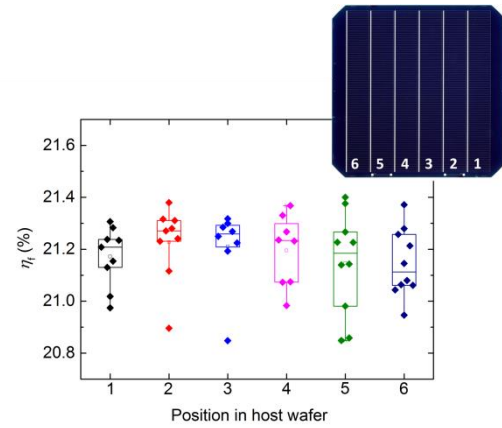


**Figure 4:** *IV* measurement results showing the designated front side energy conversion efficiency  $\eta_f$  of 54 pSPEER cells taken from different positions of the host wafers.

The currently used precursor is optimized for monofacial use. The lower  $V_{OC}$  for rear side measurement can be nearly attributed to the lower rear side  $j_{SC,des}$ . This can be verified using the one-diode model equation: The dark recombination current density  $j_{01}$  equals to  $j_{01} \approx 250 \text{ fA/cm}^2$  calculated out of the respective average front side values of  $j_{SC}$  and  $V_{OC}$  shown in Figure 3. Replacing  $j_{SC}$  front with  $j_{SC}$  rear yields a reduction of  $\Delta V_{OC} \approx 12 \text{ mV}$  which equals to the measured difference.

Higher bifaciality values for pSPEER cells can be attained by adapting the rear side optical properties and optimizing the rear side metallization fraction towards decreasing shading. The fluctuations in the  $FF$  in Fig. 3(b), can be explained by the range of the measured base resistivity of the precursors used for the fabrication.

The increase in perimeter to area ratio would suggest the importance of suppressing edge recombination [13]. Edge recombination can be shown by the rather lower pseudo-fill factor value  $\Delta pFF \approx 1.2\%_{abs}$  compared to a 6-inch bifacial solar cell. In the near future, passivating the edges can improve pSPEER solar cell performance.

#### 4 CONCLUSIONS

Bifacial shingle solar cells based on the p-type shingled passivated edge, emitter, and rear (pSPEER) cell concept are being developed and fabricated at Fraunhofer ISE. 6-inch industrial p-type Cz-Si passivated emitter rear cell (PERC) precursors are screen printed with special shingle metallization layouts to obtain six pSPEER cells per host wafer. The applied laser-assisted separation step leads to pSPEER cells of dimensions  $22 \text{ mm} \times 148 \text{ mm}$ . *IV* results of pSPEER cells show a peak designated front side energy conversion efficiency  $\eta_f = 21.4\%$  and a bifaciality factor  $\beta = 0.64$ .

By including a rear side irradiance  $G_r = 100 \text{ W/m}^2$ , the best pSPEER solar cell attains a total output power density  $p_{out} = 22.8 \text{ mW/cm}^2$ .

## ACKNOWLEDGEMENTS

The authors would like to thank all contributing colleagues at Fraunhofer ISE Photovoltaics Division who made the development of this work possible. Special thanks to Mohammad Al-Akash for measuring the pSPEER solar cells shown in this work. The work is conducted within the scope of “PV-BAT400” research project (contract no. 0324145) funded by the German Federal Ministry of Economic Affairs and Energy.

## REFERENCES

- [1] J.D.C. Dickson, “Photo-voltaic semiconductor apparatus or the like,” US Patent 2,938,938, May 31, 1960.
- [2] S. W. Glunz, J. Dicker, M. Esterle, M. Hermle, J. Isenberg, F. J. Kamerewerd, J. Knobloch, D. Kray, A. Leimenstoll, F. Lutz, D. Oßwald, R. Preu, S. Rein, E. Schäffer, C. Schetter, H. Schmidhuber, H. Schmidt, M. Steuder, C. Vorgrimler, and G. Willeke, “High-efficiency silicon solar cells for low-illumination applications,” in *29th IEEE Photovoltaic Specialists Conference New Orleans, New Orleans, 2002*, pp. 450–453.
- [3] D. Tonini, M. Bertazzo, A. Fecchio, M. Galiazzo, “Shingling Technology for Cell Interconnection: Technological Aspects and Process Integration,” *33rd EUPVSEC, Amsterdam, The Netherlands, 2017*.
- [4] R. Morad, G. Almogy, I. Suez, J. Hummel, N. Beckett, Y. Lin, D. Maydan, and J. Gannon, “Shingled solar cell module,” US 9397252 B2 US 14/594,439, Jul 19, 2016.
- [5] SunPower Corporation SunPower Introduces New Solar Panel: The Performance Series. <https://us.sunpower.com/solar-panelstechnology/p-series-solar-panels/>.
- [6] A. W. Blakers, A. Wang, A. M. Milne, J. Zhao, and M. A. Green, “22.8% efficient silicon solar cell,” *Appl. Phys. Lett.*, vol. 55, no. 13, pp. 1363–1365, 1989.
- [7] VDMA, “International Technology Roadmap for Photovoltaic: Results 2017 - Ninth Edition,” vol. 2018, <http://www.itrpv.net/Reports/Downloads/>.
- [8] P. Baliozian, E. Lohmüller, T. Fellmeth, N. Wöhrle, A. Krieg, R. Preu, “Bifacial p-type silicon shingle solar cells - the “pSPEER” concept,” *Solar RRL*, 2018.
- [9] P. Baliozian, E. Lohmüller, T. Fellmeth, N. Wöhrle, A. Krieg, R. Preu, “Bifacial Shingle Solar Cells on p-Type Cz-Si (pSPEER),” *SiliconPV 2018, AIP Conf. Proc. 1999*, 10002-1–110002-6.
- [10] M. Al-Akash, P. Baliozian, T. Fellmeth, E. Lohmüller, N. Wöhrle, R. Preu, “Metallization Fraction of Bifacial pSPEER Shingle Solar Cells,” *35th EUPVSEC, Brussels, Belgium (to be published)*.
- [11] N. Wöhrle et. al (to be submitted) 2018.
- [12] F. Fertig, S. Nold, N. Wöhrle, J. Greulich, I. Hädrich, K. Krauß, M. Mittag, D. Biro, S. Rein, and R. Preu, “Economic feasibility of bifacial silicon solar cells,” *Prog. Photovolt: Res. Appl.*, no. vol. 24, 6, pp. 800–817, 2016.
- [13] N. Wöhrle, T. Fellmeth, E. Lohmüller, P. Baliozian, A. Fell, R. Preu, “The SPEER solar cell Simulation study of shingled bifacial PERC technology based stripe cells.,” *33rd EUPVSEC, Amsterdam, The Netherlands*, pp. 844–848, 2017.
- [14] S. Werner, E. Lohmüller, P. Saint-Cast, J.M. Greulich, J. Weber, S. Maier, A. Moldovan, A.A. Brand, T. Dannenberg, S. Mack, S. Wasmer, M. Demant, M. Linse, R. Ackermann, A. Wolf, R. Preu, “Key aspects for fabrication of p-type Cz-Si PERC solar cells exceeding 22% conversion efficiency,” in *33rd EU PVSEC, Amsterdam, The Netherlands, 2017*.